

In Silico Computational Prediction of Royal Jelly Compounds as Potential Bcl-2, HER-2, and EGFR Inhibitors in Breast Cancer

Gusnia Meilin Gholam ¹, Dimas Andrianto ¹, Yelin Adalina ², I. Made Artika ^{1,*}

¹ Department of Biochemistry, Faculty of Mathematics and Natural Sciences, IPB University, Dramaga Campus, Bogor, 16680, Indonesia; gusniameilin@apps.ipb.ac.id (G.M.G.); dimasandrianto@apps.ipb.ac.id (D.A.); imart@apps.ipb.ac.id (I.M.A.);

² Research Center for Applied Botany, National Research and Innovation Agency (BRIN), Jl. Raya Jakarta-Bogor Km. 46, Cibinong, Bogor, Jawa Barat - 16911, Indonesia; yeli001@brin.go.id (Y.A.);

* Correspondence: imart@apps.ipb.ac.id;

Received: 12.11.2025; Accepted: 19.01.2026; Published: 15.02.2026

Abstract: Breast cancer remains a leading cause of cancer-related mortality worldwide, necessitating the identification of novel therapeutic targets. Royal jelly (RJ), a functional food rich in bioactive compounds, has been reported to exhibit chemopreventive properties; however, its potential molecular interactions with key breast cancer-associated target receptors, including Bcl-2, EGFR, and HER-2, remain insufficiently characterized. This study aimed to explore, at a computational level, the putative interactions between selected RJ-derived compounds and their target receptors to generate mechanistic hypotheses. Molecular docking was performed using YASARA Structure after systematic protein and ligand preparation, with structural validation assessed using Ramachandran plots. The predicted pharmacokinetic properties were evaluated using ADMET analysis. In addition, molecular dynamics (MD) simulations combined with normal mode analysis (NMA) were employed to examine the stability of the selected protein–ligand complexes. Docking analyses indicated favorable binding affinities of quercetin for Bcl-2 and naringin for EGFR and HER-2. Normal mode analysis–based simulations supported the intrinsic flexibility and favorable dynamic behavior of the docked complexes. Collectively, these *in silico* findings provide a hypothesis-generating framework suggesting that quercetin and naringin may warrant further experimental investigation as potential modulators of breast cancer-related targets. Experimental validation through *in vitro* and *in vivo* studies is required to substantiate these computational predictions.

Keywords: anti-breast cancer; molecular docking; cancer biology; molecular target identification; normal mode analysis.

© 2026 by the authors. This article is an open-access article distributed under the terms and conditions of the Creative Commons Attribution (CC BY) license (<https://creativecommons.org/licenses/by/4.0/>), which permits unrestricted use, distribution, and reproduction in any medium, provided the original work is properly cited. The authors retain copyright of their work, and no permission is required from the authors or the publisher to reuse or distribute this article, as long as proper attribution is given to the original source.

1. Introduction

Cancer is one of the most frequently diagnosed diseases, with research reports indicating a significant increase in mortality rates, particularly when the immune system is weakened. To date, extensive studies on cancer have highlighted substantial progress in medical research and therapeutic development; however, the discovery of truly curative cancer drugs remains an unfulfilled aspiration. There are now more than a hundred known types of cancer, each characterized by uncontrolled cell proliferation [1]. Among these, breast cancer

stands out as one of the most aggressive and frequently diagnosed malignancies in women, often leading to fatal outcomes [2].

Breast cancer remains a major global public health challenge, and is currently the most frequently diagnosed cancer in women worldwide. In 2022, an estimated 2.3 million women were newly diagnosed with breast cancer, with approximately 670,000 deaths reported globally, underscoring its substantial mortality burden. Breast cancer is the leading cancer among women in 157 of 185 countries, affecting populations across all geographic regions and levels of socioeconomic development. Notably, while the lifetime risk of breast cancer diagnosis is higher in countries with a very high Human Development Index (HDI), mortality rates are disproportionately higher in low-HDI countries, reflecting inequities in early detection, access to treatment, and comprehensive cancer care. Although female sex and increasing age are the strongest risk factors, nearly half of breast cancer cases occur in women without identifiable risk factors other than age and sex. These epidemiological trends highlight the urgent need for improved strategies in early diagnosis, effective treatment, and global efforts to reduce disparities in breast cancer outcomes [3].

Bcl-2 is a family of proteins that plays a crucial role in regulating apoptosis, which is a programmed cell death process. These proteins maintain a balance between cell survival and death by either inhibiting or promoting apoptosis. In many cancers, overexpression of Bcl-2 proteins allows cancer cells to survive longer and develop resistance to treatment. Consequently, developing inhibitors that specifically target Bcl-2 proteins may pave the way for more effective cancer therapies. Research focused on the design and development of Bcl-2 inhibitors aims to enhance cancer cells' sensitivity to therapeutic interventions, thereby improving the likelihood of successful treatment outcomes for cancer patients [4–7].

The epidermal growth factor receptor (EGFR) has been widely reported as a key target in anti-breast cancer drug discovery, as EGFR is often overexpressed in various types of cancers, including breast cancer [8]. The signaling pathway illustrated in Figure 1 shows that EGFR is a transmembrane protein composed of an extracellular domain (ECD) where ligand binding occurs, a transmembrane domain (TMD), and an intracellular tyrosine kinase domain responsible for the receptor's catalytic activity. The activation of EGFR triggers a cascade of downstream signaling pathways that generate mitogenic and anti-apoptotic responses. As depicted in Figure 1, one of the critical pathways involved is the phosphatidylinositol-3-kinase (PI3K) pathway, which plays a major role in tumor growth. It is important to note that EGFR belongs to the human epidermal growth factor receptor (HER) family and is also referred to as HER1. The HER family, particularly HER2, plays a vital role in the regulation of physiological cellular processes, including motility, survival, and differentiation.

Despite these advances, the discovery and optimization of multi-target agents or compounds that modulate key breast cancer-related targets, such as Bcl-2, HER-2, and EGFR, remain challenging [9]. Moreover, although functional foods and natural products, including royal jelly, have been reported to possess bioactive and chemopreventive properties, their potential molecular interactions with these critical breast cancer targets have not been systematically investigated at the atomic level. In particular, there is a lack of comprehensive *in silico* studies integrating molecular docking, pharmacokinetic prediction, and molecular dynamics simulations to explore the multi-target potential of RJ-derived compounds.

To date, no studies have reported the bioactive compounds in royal jelly (RJ) that specifically target multiple receptors such as Bcl-2, EGFR, and HER-2. Most anti-breast cancer findings have instead been reported from propolis [11,12]. According to Albalawi *et al.* [13],

oral administration of RJ at doses of 200 and 400 mg/kg produced promising antitumor effects against Ehrlich solid tumor (EST) in mice by inducing apoptosis, along with notable antioxidant and anti-inflammatory activities.

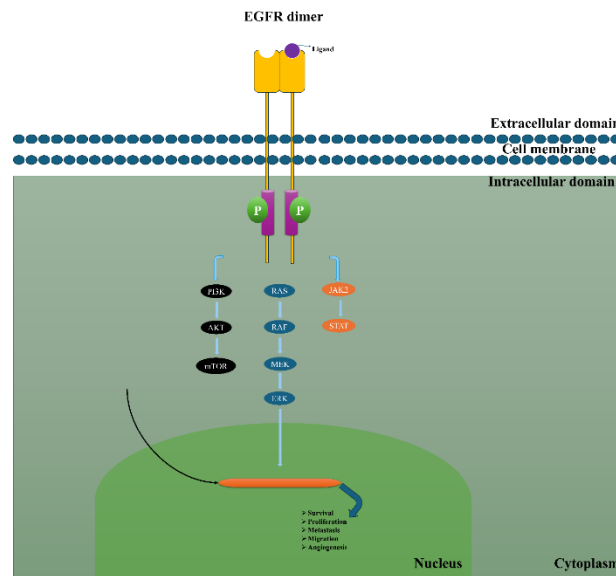


Figure 1. General overview of the EGFR signaling pathway. The illustration was adapted from Spada *et al.* [10] and recreated using Microsoft PowerPoint.

Another study by Zhang *et al.* [14] found that supplementing fermented milk containing *Lactobacillus helveticus* Lh-B02 with fresh RJ surprisingly enhanced the anti-breast cancer activity of the fermented product [14,15]. Likewise, Alnomasy *et al* [16] reported the anticancer potential of RJ using HepG2 cells. In a study exploring the bioactive components of RJ, Sirkisoon *et al.* [17] reported that HER-2 overexpression occurs in approximately 15–35% of invasive breast cancer cases and that aberrant HER-2 signaling contributes to increased metastasis and reduced patient survival. Furthermore, scientific evidence indicates that both EGFR and HER-2 are highly expressed in brain metastases from breast cancer, where these proteins play crucial roles in facilitating brain-specific metastatic spread. Preclinical and clinical studies have therefore identified EGFR and HER-2 as important therapeutic targets for female patients with breast cancer brain metastasis (BCBM). Despite these insights, no studies have yet reported the predicted mechanisms by which RJ might inhibit specific proteins, particularly those targeting Bcl-2, EGFR, and HER-2, which are considered key targets in breast cancer pathogenesis [18,19].

Among various bee products and natural matrices, RJ is distinguished by its unique biochemical composition and multifunctional biological activities. Unlike honey, propolis, or bee pollen, RJ contains a complex mixture of proteins (major royal jelly proteins/MRJPs), medium-chain fatty acids (10-hydroxy-2-decenoic acid, 10-HDA), flavonoids, and bioactive lipids that collectively modulate multiple cancer-related signaling pathways. Accumulating preclinical evidence demonstrates that RJ exhibits anti-tumour effects across diverse cancer models through mechanisms involving apoptosis induction, immune modulation, oxidative stress regulation, and epigenetic control. Importantly, RJ-derived components have been shown to directly influence molecular targets relevant to cancer progression, including apoptotic regulators (e.g., Bcl-2 and p53), inflammatory mediators (e.g., NF- κ B), epigenetic enzymes (e.g., histone deacetylases, HDACs), and key survival pathways (e.g., PI3K/AKT). These multi-target activities align well with current therapeutic paradigms that emphasize pathway convergence rather than single-target inhibition. Furthermore, RJ has demonstrated

favorable safety and tolerability profiles in preclinical and limited clinical settings, particularly as a supportive agent during cancer therapy [20].

RJ is widely recognized for its ability to support various physiological functions naturally. Beyond enhancing memory and promoting digestive health, RJ also shows therapeutic potential in preventing or alleviating symptoms of degenerative diseases such as Alzheimer's. The diverse range of bioactive compounds present in RJ makes it a promising candidate for treating chronic conditions, including cancer and aging-related disorders. Its use in cosmetic formulations has also increased due to its skin-rejuvenating properties and ability to slow down the aging process [15]. Despite these well-documented health benefits, no research to date has explored RJ's anticancer potential through direct targeting of the Bcl-2, EGFR, and HER-2 receptors. Therefore, this study aims to investigate the bioactive compounds in RJ as potential novel inhibitors of Bcl-2, EGFR, and HER-2 receptors for the treatment of breast cancer.

2. Materials and Methods

2.1. Receptor selection and structural preparation.

The Bcl-2 protein with a resolution of 2.10 Å, the EGFR protein with a resolution of 2.60 Å, and the HER-2 protein with a resolution of 3.21 Å were downloaded in (.pdb) format from the RCSB Protein Data Bank, with respective PDB codes 2W3L (rcsb.org/structure/2W3L [21]) [18], 1M17 (rcsb.org/structure/1M17 [22]), and 3RCD (rcsb.org/structure/3RCD [23]). Protein preparation was performed using YASARA Structure [24], in which hydrogen atoms were added, and water molecules were removed. Subsequently, all three proteins underwent energy minimization, and the final structures were saved again in (.pdb) format. In this study, the quality of the prepared Bcl-2, EGFR, and HER-2 proteins was further evaluated using Ramplot (ramplot.in/) [25]. The overall research workflow is presented in Figure 2.

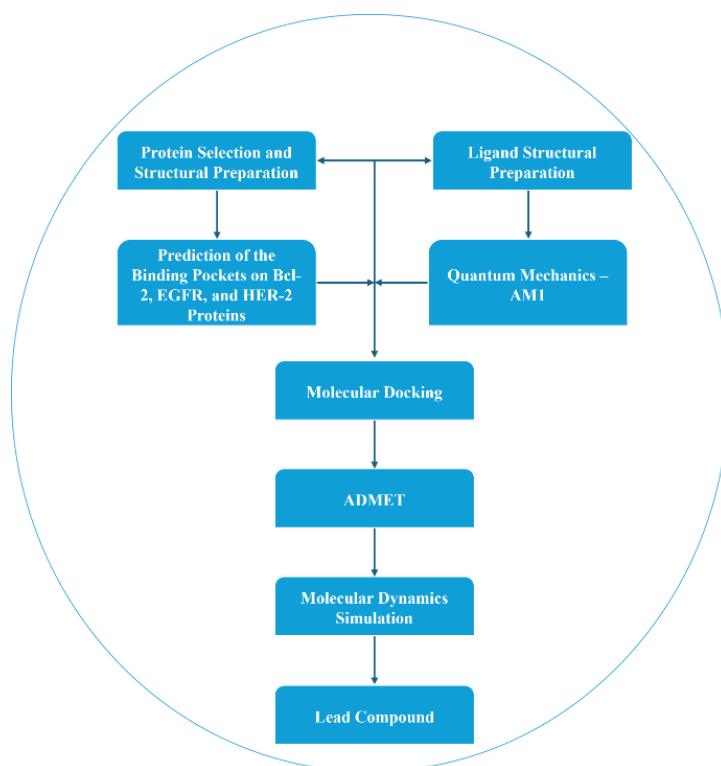


Figure 2. The workflow of this study was designed to propose potential new anti-breast cancer drug candidates.

2.2. Prediction of the pocket on receptor Bcl-2, EGFR, and HER-2.

The binding sites of the Bcl-2, EGFR, and HER-2 receptors were predicted using the open-access COACH server (zhanggroup.org/COACH/). The previously prepared receptor structures of Bcl-2, EGFR, and HER-2 were uploaded to the server for binding site prediction [26,27].

2.3. Ligand structural preparation.

The list of bioactive compounds from RJ was obtained from El-Seedi *et al.* [28] and Botezan *et al.* [29], and their 3D structures were downloaded from PubChem (pubchem.ncbi.nlm.nih.gov/) in (.sdf) format. The RJ compounds were selected based on their reported bioactive properties and documented biological activities in the literature. The 3D structures of the bioactive compounds were then prepared using YASARA Structure with the quantum mechanics (QM) AM1 (QM-AM1) approach, followed by energy minimization. Prior to applying these techniques, a “clean-all” operation was performed to add hydrogen atoms. The final 3D structures were saved in the format (*_ligands.sdf) for subsequent molecular docking analysis [24]. Ligand structures were prepared using a QM-based approach to optimize geometries and accurately describe electronic properties prior to molecular docking. This QM treatment accounts for electronic polarization and charge distribution effects, thereby improving the reliability of subsequent receptor–ligand interaction analyses [30].

2.4. Molecular docking.

Molecular docking was performed using YASARA Structure by applying the VINA method embedded within the dock_runscreening macro. The docking simulations were executed using the AMBER14 force field. First, the Bcl-2, EGFR, and HER-2 protein structures in (.pdb) format were uploaded into YASARA for docking, with the proteins set as rigid and saved in the (*receptor.sce) format. Docking simulations were performed under a rigid-receptor approximation, with protein structures prepared by adding missing hydrogen atoms and assigning partial charges using the AMBER14 force field to ensure chemically consistent geometries prior to docking [31,32]. Additionally, a specific grid box was defined for each protein target, as illustrated in Figure 3. The grid box was defined to fully encompass the entire target receptor, allowing the ligand to naturally interact with all potential amino acid residues of the receptor. Next, the bioactive RJ compounds in (ligands.sdf) format were uploaded into YASARA, and the Bcl-2 protein, along with the RJ ligands, were saved as (_complex.sce). Finally, the prepared dock_runscreening macro was employed to execute the molecular docking simulations [24,33,34].

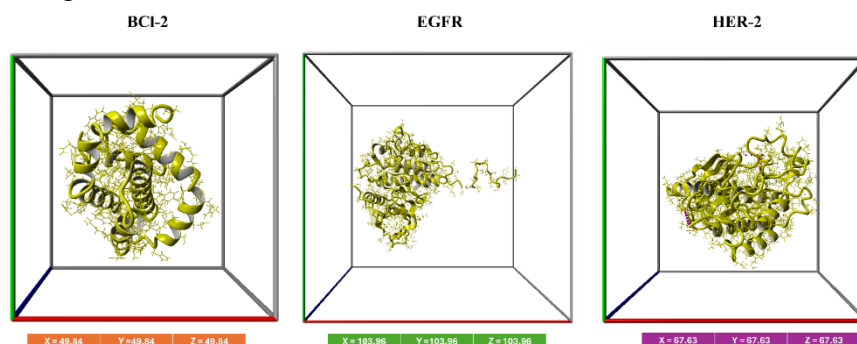


Figure 3. Proteins were kept in a rigid state, and the grid box dimensions used during the docking process are shown. The visualization was generated using YASARA.

2.5. ADMET analysis.

The bioactive compounds selected from the molecular docking analysis were further profiled for absorption, distribution, metabolism, elimination, and toxicity (ADMET) using the pkCSM online tool (biosig.lab.uq.edu.au/pkcsm/). During the process, each bioactive compound was individually submitted to the pkCSM server, utilizing the SMILES data obtained from PubChem [35].

2.6. Molecular dynamics simulation.

Molecular dynamics (MD) simulations were performed to assess the deformability and rigidity of the selected inhibitor–protein complexes using the iMODS server (imods.iqfr.csic.es/), which is based on normal mode analysis (NMA). Prior to running the MD simulations, each protein underwent energy minimization using YASARA [27,28]. Subsequently, the complexes in (.pdb) format were processed and analyzed through the iMODS server [36–38].

3. Results and Discussion

3.1. Post-preparation analysis.

The prepared Bcl-2 receptor was evaluated for structural quality using the Ramachandran plot. Figures 4A–C present the visualization of the analysis generated using Ramplot. The results revealed that amino acid residues within the favored region accounted for 88.489%, while those in the allowed region accounted for 10.072%. These findings indicated that the Bcl-2 protein was in good structural condition, with only 1.439% of residues in the disallowed region.

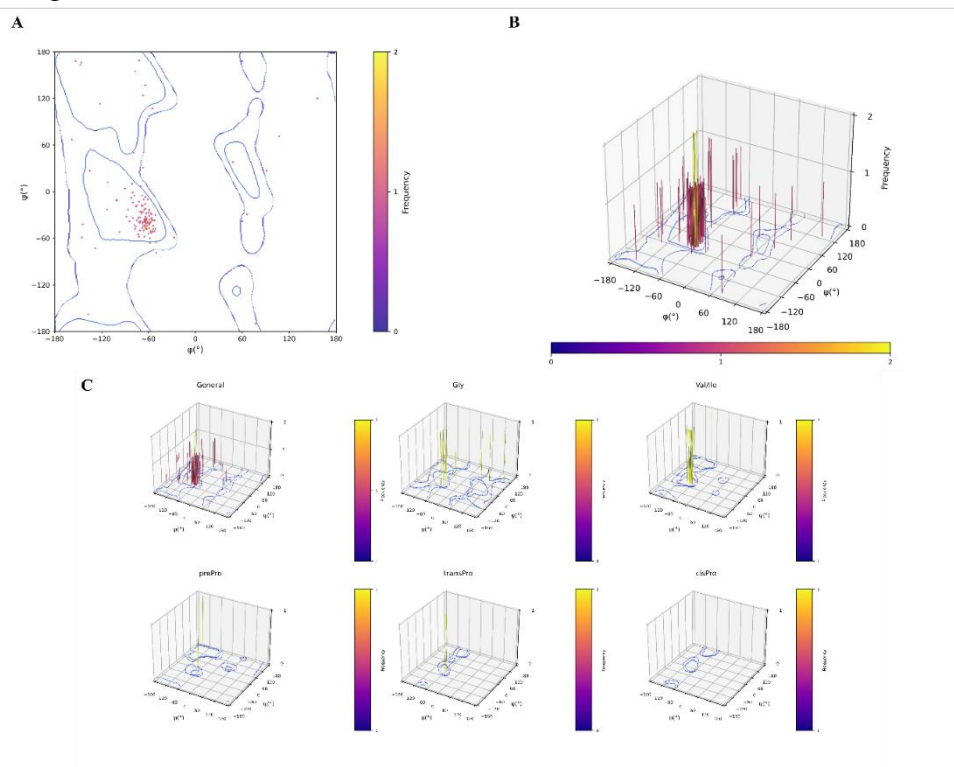


Figure 4. Ramachandran plot of the structural quality of the prepared Bcl-2 receptor: (a) 2D Ramachandran Heat Map; (b) Standard 3D Ramachandran plot; (c) 3D Ramachandran plot of six distinct categories: general case (Ala and remaining 15 amino acids), Gly, Val/Ile, pre-Pro, trans-Pro, and cis-Pro.

Figures 5A–C display the quality assessment of the prepared EGFR protein, which showed that 90.584% of residues were located in the favored region, with only 2.273% in the disallowed region, confirming that EGFR was also well-prepared. Similarly, Figures 6A–C illustrate the quality of the HER-2 protein after preparation, showing that 90.406% of residues were in the favored region, while only 2.583% were in the disallowed region.

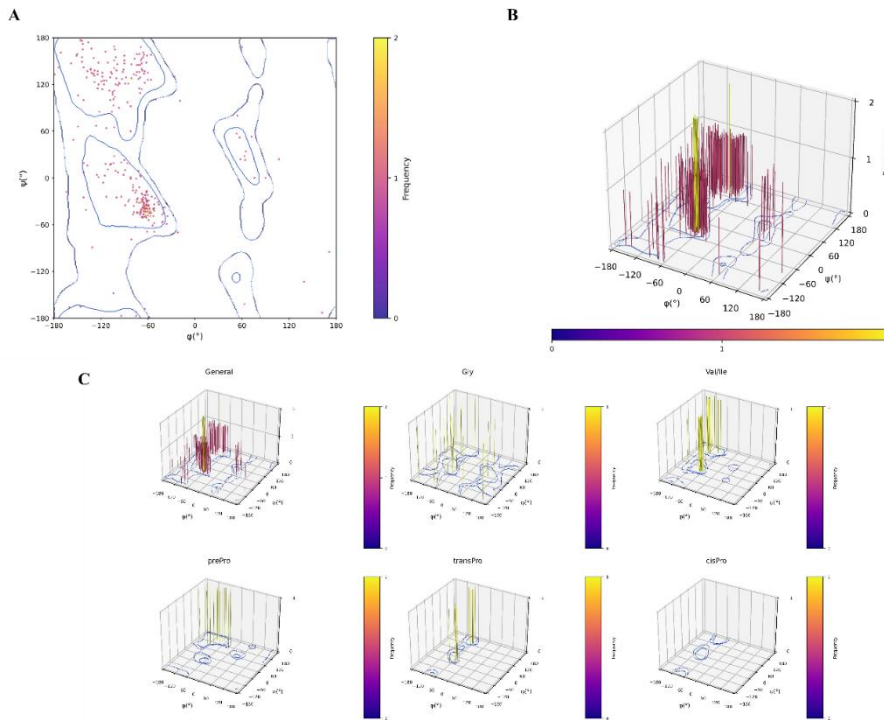


Figure 5. Ramachandran plot of the structural quality of the prepared EGFR receptor: (a) 2D Ramachandran Heat Map; (b) Standard 3D Ramachandran plot; (c) 3D Ramachandran plot of six distinct categories: general case (Ala and remaining 15 amino acids), Gly, Val/Ile, pre-Pro, trans-Pro, and cis-Pro.

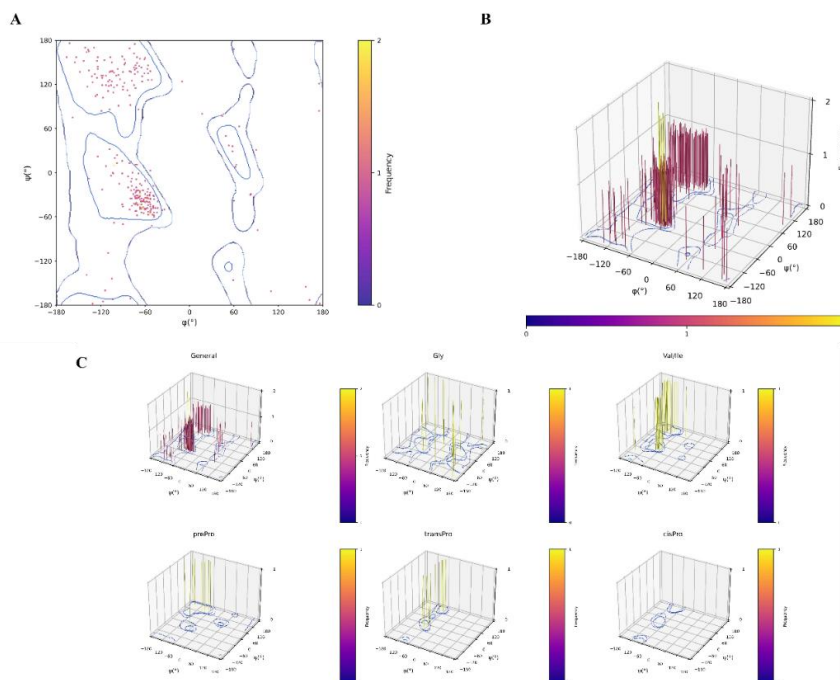


Figure 6. Ramachandran plot of the structural quality of the prepared HER-2 receptor: (a) 2D Ramachandran Heat Map; (b) Standard 3D Ramachandran plot; (c) 3D Ramachandran plot of six distinct categories: general case (Ala and remaining 15 amino acids), Gly, Val/Ile, pre-Pro, trans-Pro, and cis-Pro.

Overall, all three proteins—Bcl-2, EGFR, and HER-2—demonstrated favored region percentages exceeding 88%, confirming proper and accurate preparation. According to [39], a protein model is considered of good quality when more than 85–90% of its residues are located in the favored region of the Ramachandran plot. Therefore, the prepared Bcl-2, EGFR, and HER-2 proteins met this quality standard, validating that they were in optimal condition for further computational analysis. The application of Ramachandran plot analysis in cancer studies has also been reported by Turpo-Pequeña *et al.* [40], who used it to assess the PARP-1 protein model in a study of triple-negative breast cancer.

3.2. Binding site analysis.

Figure 7 presents the predicted binding sites generated using the COACH server. The potential binding sites of the Bcl-2 protein were identified at residues 38, 39, 42, 43, 46, 47, 50, 53, 54, 67, 68, 71, 72, 74, 75, 78, 79, 80, 81, 83, 84, 88, 136, and 137. For the EGFR protein, the predicted binding site residues include 23, 24, 25, 31, 48, 50, 80, 95, 96, 97, 98, 99, 101, 102, 146, 147, 149, 159, and 160. Meanwhile, for the HER-2 protein, the residues identified as binding sites were 17, 18, 19, 25, 42, 44, 70, 85, 86, 87, 88, 89, 91, 92, 136, 137, 139, 149, and 150. These predictions were utilized in this study to analyze the molecular docking results. According to Mushebenge *et al.* [41], predicting the binding sites of drug candidates on a target protein provides valuable insight into their potential and effectiveness. This technique has proven instrumental in enabling researchers to explore and evaluate drug–target interactions at the molecular level, thereby accelerating the drug discovery process.

Beyond the identification of binding-site residues, the predicted pockets on Bcl-2, EGFR, and HER-2 represent structurally and functionally relevant regions known to accommodate small-molecule ligands that modulate apoptotic signaling and receptor-mediated pathways. Accurate prediction of these putative binding sites is critical for rational drug design, as it enables the positioning of candidate compounds within energetically favorable cavities and facilitates the assessment of ligand–receptor complementarity at the molecular level. By integrating three-dimensional structural information, binding site prediction supports the evaluation of binding geometry and interaction feasibility, thereby strengthening the biological plausibility of subsequent docking results. Importantly, reliable identification of ligand-accessible regions on therapeutically relevant targets such as Bcl-2, EGFR, and HER-2 provides a foundational framework for understanding how bioactive compounds may influence protein function and downstream signaling pathways, which is essential for hypothesis generation in early-stage drug discovery [42–44].

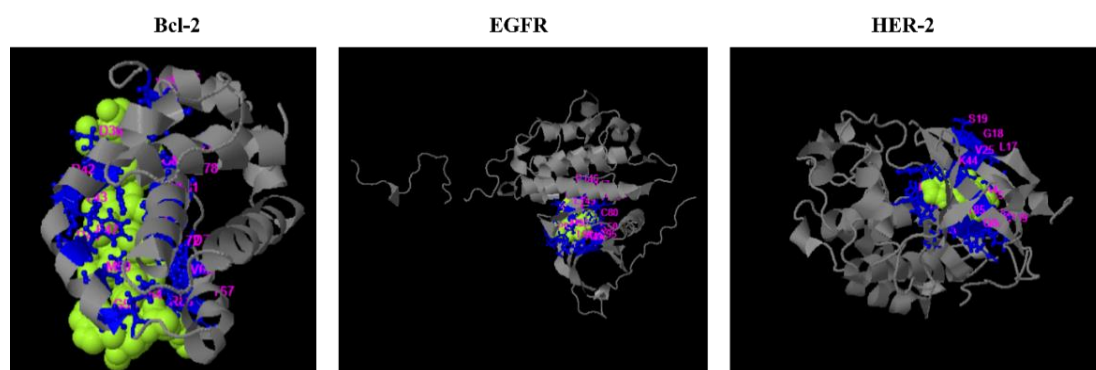


Figure 7. The pocket containing amino acid residues predicted by COACH to be the active site. Binding site prediction visualized using COACH.

3.3. Post-docking analysis.

Bioactive compounds from RJ were docked against the Bcl-2 protein using the VINA method. The results indicated that the top-ranked compound based on binding affinity (kcal/mol) was venetoclax, which served as a control to establish a benchmark for binding energy values and Bcl-2 amino acid residue interactions. Notably, the RJ bioactive compound quercetin ranked second, *with a binding energy comparable to that of venetoclax* at 8.129 kcal/mol (Table 1).

Table 1. Results of post-docking analysis: binding affinities for the Bcl-2 target.

Rank	CID	Compound	Binding energy (Kcal/mol)
1	49846579	Venetoclax (Control drug)	8.658
2	5280343	Quercetin	8.129
3	442428	Naringin	8.116
4	439246	Naringenin	7.63
5	5281707	Coumestrol	7.624
6	5280961	Genistein	7.568
7	5280378	Formononetin	7.484
8	11404337	Obatoclax (Control drug)	7.185
9	5281616	Galangin	7.089
10	1794427	Chlorogenic Acid	7.025
11	5281607	Chrysin	6.977
12	689043	Caffeic Acid	6.841
13	72281	Hesperetin	6.51
14	445858	Ferulic Acid	5.697
15	5312738	10-Hydroxy-2-decenoic acid	5.075

Docking scores were used to estimate the relative binding affinity and binding modes of ligands toward the target receptors rather than to determine inhibitory function directly. Therefore, the docking results presented in this study provide predictive insights into ligand–receptor interactions and should be further validated through molecular dynamics simulations to assess the stability and dynamic behavior of the complexes [45].

Post-docking analysis of binding energies targeting the EGFR protein is presented in Table 2. The results show that venetoclax exhibited the strongest binding affinity, followed by naringin, quercetin, chrysin, and galangin. These four compounds demonstrated binding energies superior to obatoclax, which was used as the drug control, with values ranging from 8.224 to 8.734 kcal/mol.

Table 2. Binding energy values from post-docking analysis targeting the EGFR receptor.

Rank	CID	Compound	Binding energy (Kcal/mol)
1	49846579	Venetoclax (Drug repurposing)	10.749
2	442428	Naringin	8.734
3	5280343	Quercetin	8.487
4	5281607	Chrysin	8.306
5	5281616	Galangin	8.224
6	11404337	Obatoclax (Drug repurposing)	8.223
7	72281	Hesperetin	8.192
8	5281707	Coumestrol	8.189
9	439246	Naringenin	7.998
10	5280961	Genistein	7.812
11	1794427	Chlorogenic Acid	7.707
12	5280378	Formononetin	7.452
13	689043	Caffeic Acid	6.335
14	445858	Ferulic Acid	6.202
15	5312738	10-Hydroxy-2-decenoic acid	5.053

Table 3 presents the binding energies and rankings of RJ bioactive compounds targeting the HER-2 protein. The results again showed that venetoclax, the control drug, had the highest binding affinity, followed by naringin and hesperetin, with values of 9.125 and 8.677 kcal/mol, respectively. Both of these compounds exhibited stronger binding energies than the obatoclax control.

Table 3. Binding energy values from post-docking analysis targeting the HER-2 receptor.

Rank	CID	Compound	Binding energy (Kcal/mol)
1	49846579	Venetoclax (Drug repurposing)	10.717
2	442428	Naringin	9.125
3	72281	Hesperetin	8.677
4	11404337	Obatoclax (Drug repurposing)	8.669
5	5281607	Chrysin	8.64
6	439246	Naringenin	8.421
7	5280343	Quercetin	8.374
8	5281616	Galangin	8.28
9	5280961	Genistein	8.088
10	5281707	Coumestrol	7.937
11	1794427	Chlorogenic Acid	7.873
12	5280378	Formononetin	7.636
13	689043	Caffeic Acid	6.528
14	445858	Ferulic Acid	6.262
15	5312738	10-Hydroxy-2-decenoic acid	5.343

Therefore, based on the comparative binding energy analysis, lead bioactive compounds have been identified for each target protein for further investigation. The selected RJ bioactive compounds for the Bcl-2 protein were quercetin, naringin, naringenin, coumestrol, genistein, and formononetin. For the EGFR target, the selected compounds were naringin, quercetin, chrysin, and galangin; for the HER-2 target, the selected compounds were naringin and hesperetin.

The interaction analysis presented in Figure 8A illustrates the Bcl-2–Venetoclax complex, in which Venetoclax engages in seven types of interactions. Hydrogen bonds were observed between Venetoclax and the amino acid residues Glu95, Tyr67, Arg105, Ala59, Gly104, and Asn102 of the Bcl-2 protein. In contrast, quercetin forms hydrogen bonds with the residues Ala72, Ser75, Asn122, Arg26, Ser64, and Lys22 of Bcl-2. Notably, quercetin interacts with residues 72 and 75, which are located within the predicted binding site from the COACH analysis, indicating a favorable interaction with the Bcl-2 pocket (Figure 8B).

For the Bcl-2–naringin complex, as shown in Figure 8C, hydrogen bonds were observed with residues Gln25, Arg26, Asp61, Ser64, and Asn122, accompanied by hydrophobic interactions that contribute to the stability of the complex. Figure 8D depicts two hydrogen bonds and several π -type interactions, including π -cation, π -anion, and π -alkyl bonds, formed between naringenin and the aromatic rings of Bcl-2. Similar interaction patterns were also observed in Figure 8E for the Bcl-2–coumestrol complex.

Interestingly, genistein exhibited an unfavorable acceptor–acceptor interaction with residue Glu111 in the Bcl-2–genistein complex (Figure 8F), which may affect its binding stability. Meanwhile, the Bcl-2–formononetin complex (Figure 8G) demonstrated the presence of hydrogen bonding, hydrophobic interactions, and π -anion interactions, all of which contribute to the overall stability of the complex.

In the EGFR–ligand complexes presented in Figure 9, Venetoclax was observed to interact with the EGFR receptor through hydrogen bonds, hydrophobic interactions, as well as π -cation and π -anion interactions (Figure 9A). Among all test ligands, only quercetin formed

a π -cation interaction. The remaining four test ligands consistently formed hydrophobic interactions and hydrogen bonds (Figures 9B–9E).

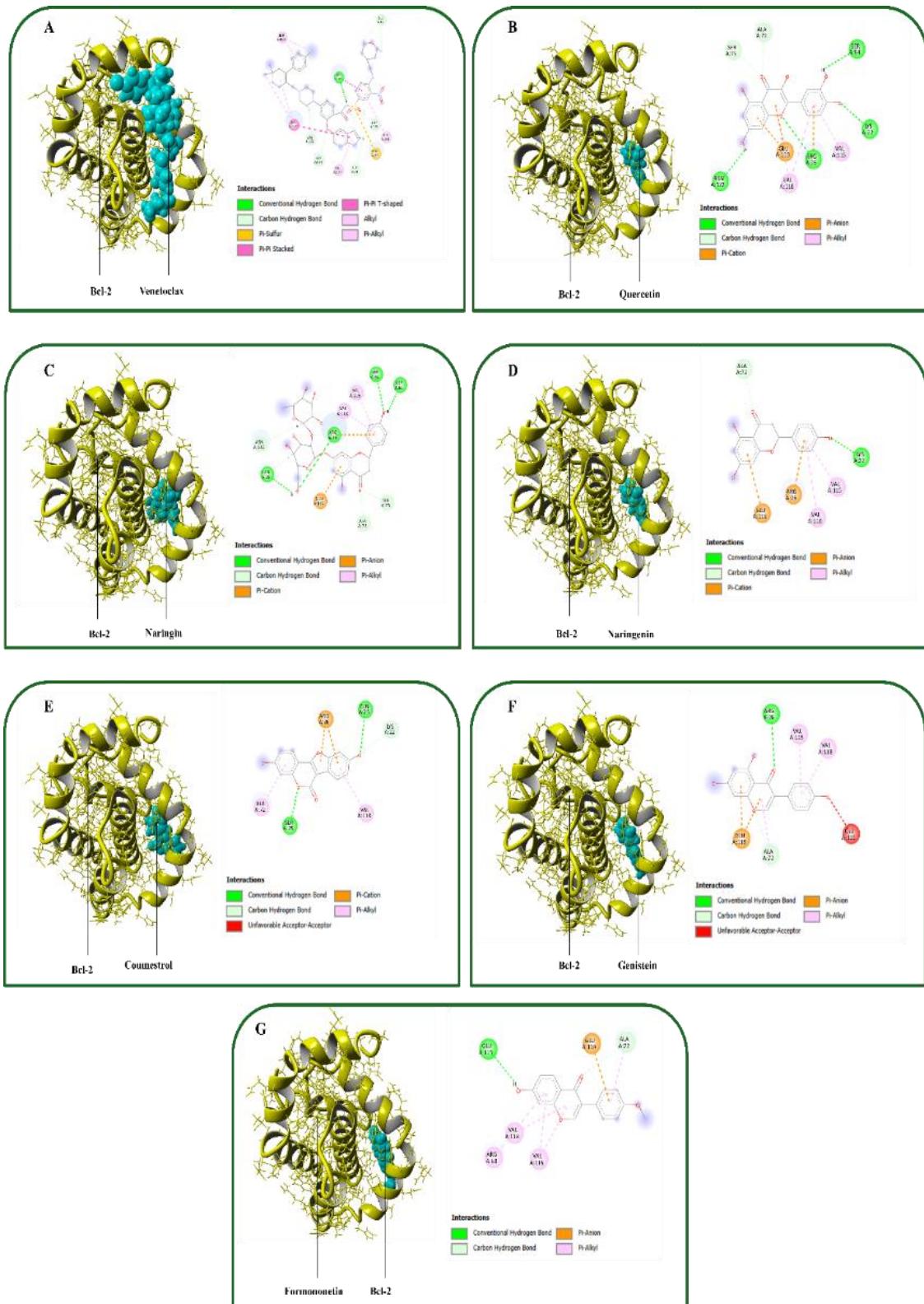


Figure 8. 2D and 3D visualization of the selected Bcl-2–ligand complexes: (a) Bcl-2–venetoclax complex; (b) Bcl-2–quercetin complex; (c) Bcl-2–naringin complex; (d) Bcl-2–naringenin complex; (e) Bcl-2–coumestrol complex; (f) Bcl-2–genistein complex; (g) Bcl-2–formononetin complex.

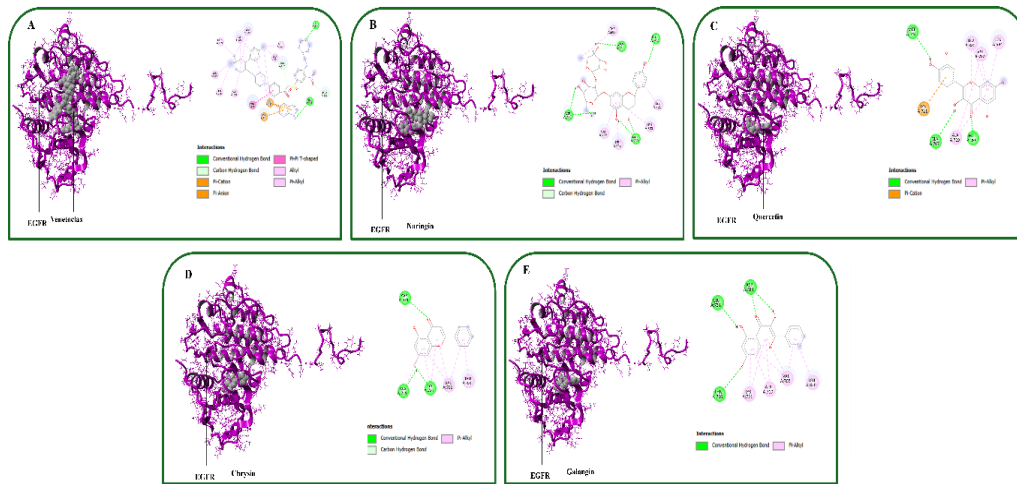


Figure 9. 2D and 3D visualization of the selected EGFR–ligand complexes: (a) EGFR–venetoclax complex; (b) EGFR–naringin complex; (c) EGFR–quercetin complex; (d) EGFR–chrysin complex; (e) EGFR–galangin complex.

In the HER-2 ligand complexes, Venetoclax exhibited a diverse range of interactions (Figure 10A). Naringin also interacted effectively with HER-2, displaying similar interaction types as Venetoclax (Figure 10B). However, the study indicated that hesperetin interacted poorly with the HER-2 receptor due to an unfavorable acceptor–acceptor interaction at SER783 (Figure 10C).

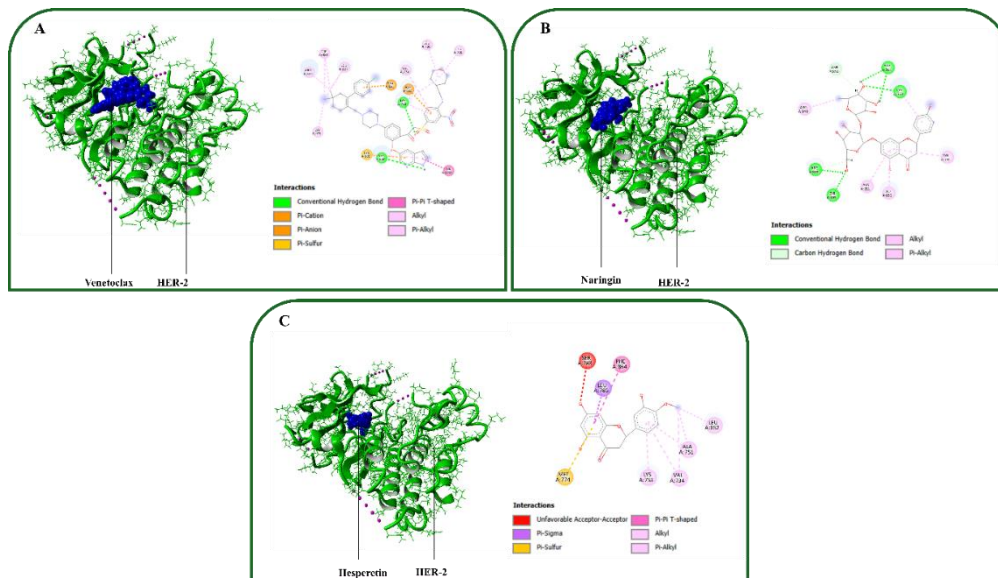


Figure 10. 2D and 3D visualization of the HER-2–ligand complexes: (a) HER-2–venetoclax complex; (b) HER-2–naringin complex; (c) HER-2–hesperetin complex.

Venetoclax and Obatoclax were not employed as target-specific inhibitors for EGFR or HER-2. Instead, these compounds were included as reference molecules within a drug repurposing framework to comparatively evaluate their potential binding behavior across multiple cancer-related targets. Notably, although Venetoclax and Obatoclax are established Bcl-2 family inhibitors, their well-characterized molecular structures and clinical relevance allow exploratory *in silico* assessment against EGFR and HER-2, without implying canonical target specificity or therapeutic equivalence [46–49]. In cancer research, drug repurposing aims to identify existing drugs with established safety profiles for new anticancer indications,

thereby accelerating therapeutic development. This strategy significantly reduces time, cost, and risk compared to de novo drug discovery while enabling rapid clinical translation. The integration of advanced computational approaches, multi-omics technologies, and artificial intelligence further enhances the identification of novel drug–target interactions. Collectively, drug repurposing represents a practical and impactful approach to address unmet clinical needs in cancer therapy [50,51].

Post-docking analysis demonstrated that the selected ligands formed stable complexes with the target receptors Bcl-2, HER-2, and EGFR through a combination of hydrogen bonding and hydrophobic interactions. These non-covalent interactions contributed to favorable binding orientations and energetically preferred conformations within the respective binding pockets, supporting the stability of the ligand–receptor complexes. Similar interaction patterns, particularly hydrophobic and π -related interactions, have been widely reported in previous molecular docking studies involving Bcl-2, HER-2, and EGFR, highlighting their critical role in enhancing binding affinity and complex stabilization. The predicted binding sites for Bcl-2, HER-2, and EGFR were located within well-defined cavities known to accommodate small-molecule inhibitors. These regions are enriched with amino acid residues capable of forming complementary electrostatic and hydrophobic contacts with the ligands, thereby supporting the reliability of the binding site prediction. The observed binding site characteristics and interaction profiles are consistent with those described in related *in silico* studies targeting these receptors, reinforcing the biological relevance of the identified binding regions and their potential role in modulating receptor activity [46,52,53].

3.4. ADMET analysis.

ADMET profiling was performed using pkCSM to evaluate the pharmacokinetic and safety-related properties of the selected compounds. According to pkCSM criteria, a human intestinal absorption (HIA) value of 70–100% indicates good absorption, whereas values below 30% are considered low [54]. Quercetin demonstrated good predicted intestinal absorption (HIA = 77.207%) and favorable safety parameters, including no hERG II inhibition and no hepatotoxicity. In contrast, naringin exhibited low predicted intestinal absorption (HIA = 25.796%), suggesting potential limitations in oral bioavailability despite its acceptable safety profile. Therefore, while both compounds showed promising *in silico* interaction and safety characteristics, their pharmacokinetic limitations—particularly the low intestinal absorption of naringin—necessitate cautious interpretation of their therapeutic potential and highlight the need for formulation strategies or further experimental validation. All predicted ADMET results are presented in Table 4.

It should be noted that all ADMET parameters reported in this study were derived from *in silico* computational predictions using pkCSM. While such approaches are valuable for early-stage pharmacokinetic and safety screening, they do not fully capture the complexity of *in vivo* biological systems. Therefore, experimental validation through appropriate *in vitro* and *in vivo* pharmacokinetic studies is required to confirm the predicted absorption, distribution, metabolism, and toxicity profiles. Future experimental investigations will be essential to improve the accuracy and translational relevance of the present findings.

Table 4. ADMET profile of the selected inhibitor candidates for each target protein.

Compound	Receptor Target	Intestinal absorption (human) (%)	BBB permeability (log BB)	CYP2C9 inhibitor	CYP2D6 inhibitor	Total clearance (log ml/min/kg)	AMES Toxicity	Hepatotoxicity
Venetoclax (Control drug)	-	100	-1.747	No	No	-0.096	No	Yes
Quercetin	Bcl-2 and EGFR	77.207	-1.098	No	No	0.407	No	No
Naringin	Bcl-2, EGFR, and HER-2	25.796	-1.6	No	No	0.318	No	No
Naringenin	Bcl-2	91.31	-0.578	No	No	0.06	No	No
Coumestrol	Bcl-2	92.472	-0.099	Yes	No	0.651	Yes	No
Genistein	Bcl-2	93.387	-0.71	No	No	0.151	No	No
Formononetin	Bcl-2	96.112	0.157	Yes	No	0.258	No	No
Chrysin	EGFR	93.761	0.047	Yes	No	0.405	No	No
Galangin	EGFR	93.985	-0.748	Yes	No	0.256	No	No
Hesperetin	HER-2	70.277	-0.719	No	No	0.044	No	No

3.5. Post-molecular dynamics analysis.

To evaluate the intrinsic flexibility and collective motions of the Bcl-2 (Figure 11A), EGFR (Figure 12A), and HER-2 (Figure 13A) complexes, this study employed normal mode analysis (NMA) using the iMODS server. This approach provides insights into the low-frequency, large-scale motions of protein–ligand complexes around their near-equilibrium conformations. All NMA-derived dynamic analyses are presented in Figures 11–13.

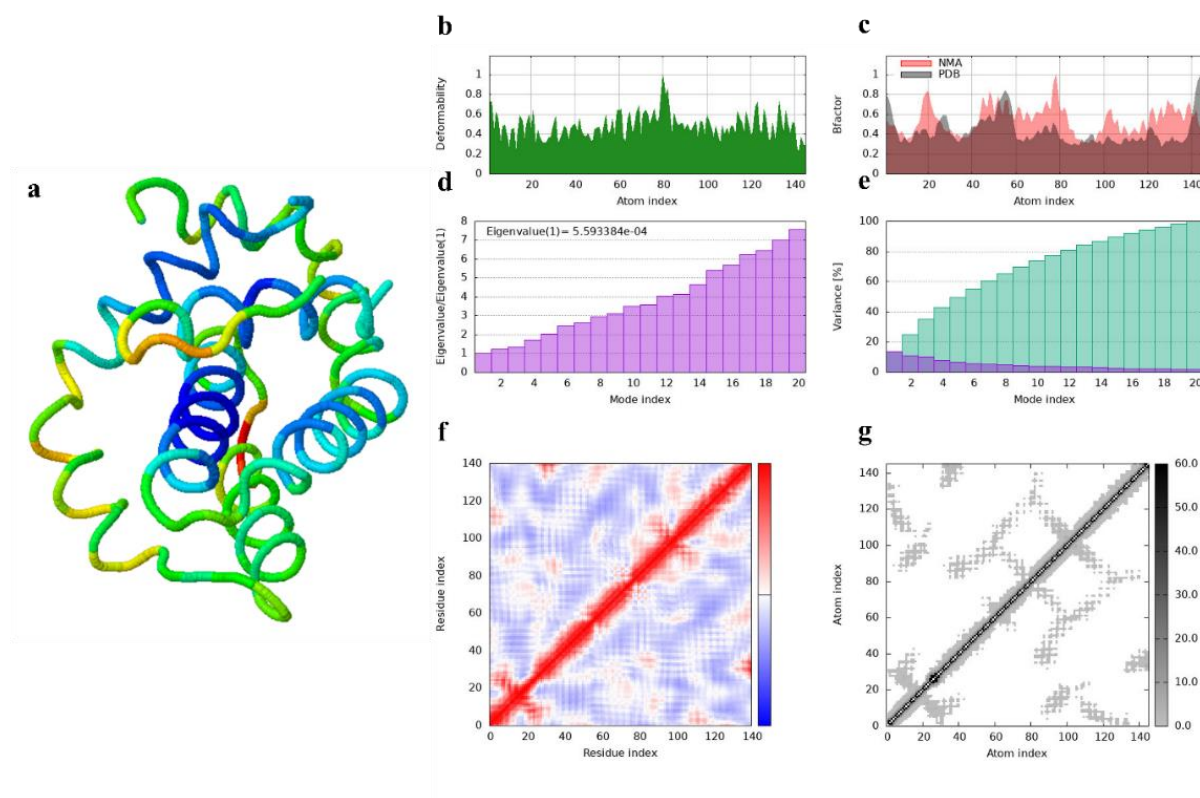


Figure 11. Molecular dynamics simulation using the normal mode analysis (NMA) technique for the Bcl-2-quercetin complex. Visuals and plots were generated using iMODS: (a) NMA mobility; (b) Deformability; (c) B-factor values; (d) Eigenvalues; (e) Variance; (f) Co-variance map; (g) Elastic network.

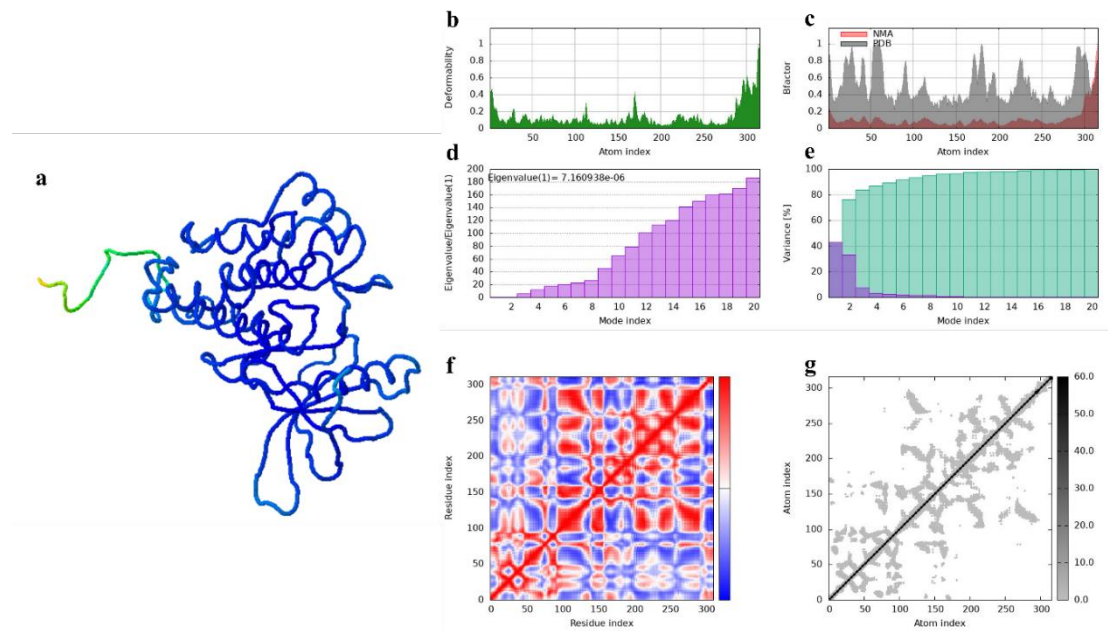


Figure 12. Molecular dynamics simulation using the normal mode analysis (NMA) technique for the EGFR-naringin complex. Visuals and plots were generated using iMODS: (a) NMA mobility; (b) Deformability; (c) B-factor values; (d) Eigenvalues; (e) Variance; (f) Co-variance map; (g) Elastic network.

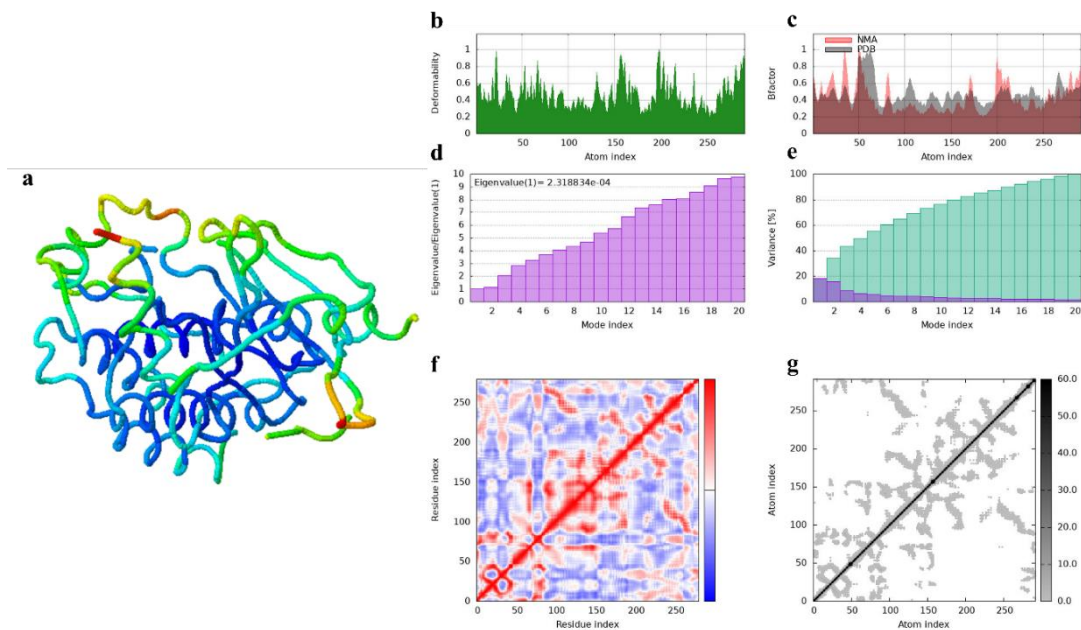


Figure 13. Molecular dynamics simulation using the normal mode analysis (NMA) technique for the HER-2-naringin complex. Visuals and plots were generated using iMODS: (a) NMA mobility; (b) Deformability; (c) B-factor values; (d) Eigenvalues; (e) Variance; (f) Co-variance map; (g) Elastic network.

As reported by Bauer *et al.* [55], NMA enables the identification of the dominant conformational modes accessible to a protein at its minimum-energy state, offering a computationally efficient approximation of collective motions without the time-dependent sampling characteristic of classical molecular dynamics simulations.

Deformability analysis was conducted to assess regions of relative flexibility that may influence protein function. As shown in Figure 11B, the Bcl-2 complex exhibited moderate deformability, while EGFR displayed relatively lower deformability fluctuations (Figure 12B). In contrast, HER-2 showed comparatively higher deformability peaks (Figure 13B), suggesting

greater intrinsic flexibility within specific regions of the protein structure. These observations reflect relative conformational tendencies rather than definitive structural stability.

The corresponding B-factor profiles derived from NMA (Figures 11C–13C) were consistent with the deformability trends, with regions of higher predicted flexibility exhibiting higher B-factor amplitudes. Since NMA-derived B-factors are proportional to root mean square fluctuations, they provide a qualitative measure of atomic displacement within the harmonic approximation [38,56,57].

Eigenvalue analysis further supported these observations, with the Bcl-2, EGFR, and HER-2 complexes exhibiting eigenvalues of 5.593384×10^{-4} (Figure 11D), 7.160938×10^{-6} (Figure 12D), and 2.318834×10^{-4} (Figure 13D), respectively. Lower eigenvalues indicate reduced energetic requirements for collective deformation, reflecting relative flexibility rather than absolute stability. The variance plots (Figures 11E–13E) illustrate the distribution of motion across individual and cumulative modes.

Covariance matrices (Figures 11F–13F) revealed patterns of correlated, uncorrelated, and anti-correlated residue motions, providing insight into cooperative domain movements within each complex. In addition, elastic network models (Figures 11G–13G) highlighted regions of relative rigidity and flexibility, where darker connections represent stiffer inter-residue constraints [38,56,58]. Overall, NMA using iMODS offers a qualitative framework for understanding slow collective motions and intrinsic flexibility of protein–ligand complexes. For example, the study by Alsedfy et al. [38] investigated the stability and slow dynamics of cur-IONPs/protein-docked complexes and employed NMA as part of their *in silico* drug design approach.

To clearly distinguish between classical molecular dynamics (MD) simulations and normal mode analysis (NMA), it is important to note that these approaches address protein dynamics at different levels. Classical MD simulations were employed to evaluate the time-dependent stability and atomistic interactions of the protein–ligand complexes under explicit force-field-based conditions. In contrast, NMA was applied as a complementary, computationally efficient approach to investigate the intrinsic collective motions and global flexibility of the protein–ligand complexes around their equilibrium conformations. In this study, NMA was performed using the iMODS server, which conducts enhanced normal mode analysis in internal coordinates. This method enables the assessment of large-scale, biologically relevant motions without relying on long-timescale MD trajectories. The iMODS analysis provided insights into protein deformability, eigenvalues, B-factors, variance maps, and residue–residue covariance matrices, thereby offering a mechanistic interpretation of the structural flexibility and dynamic behavior of the docked complexes. Collectively, classical MD simulations and NMA were used in a complementary manner: MD simulations assessed local stability and interaction persistence over time, whereas NMA elucidated global motion patterns and conformational adaptability, strengthening the interpretation of protein–ligand dynamics within a hypothesis-generating computational framework [38,58–61].

Bcl-2, EGFR, and HER-2 operate within highly interconnected signaling networks that regulate apoptosis, proliferation, and cell survival; therefore, the predicted ligand–receptor interactions observed in this study should not be interpreted as direct or isolated pathway inhibition. Given the pleiotropic nature of polyphenolic compounds such as quercetin and naringin, potential off-target effects cannot be excluded and may contribute to both their biological activities and pharmacokinetic limitations. Accordingly, these *in silico* results are

intended as hypothesis-generating insights that require further experimental validation to clarify pathway-level effects and target specificity.

4. Conclusions

This study presents an *in silico* computational approach to propose potential molecular interactions targeting the Bcl-2, EGFR, and HER-2 proteins in breast cancer. All three proteins exhibited high structural quality as assessed by Ramachandran plot analysis and were subjected to molecular docking using AutoDock Vina, with bioactive compounds derived from royal jelly (RJ) as test ligands. The docking results showed that quercetin exhibited a binding energy comparable to that of the control drug venetoclax for the Bcl-2 protein, while naringin demonstrated the strongest binding affinity toward both EGFR and HER-2. ADMET profiling predicted that quercetin and naringin possess favorable drug-like properties, suggesting their potential as promising lead compounds. Furthermore, complex stability analyses based on normal mode analysis (NMA) indicated intrinsic flexibility and favorable dynamic behavior of the docked complexes. Overall, this study does not claim definitive drug candidacy; rather, it proposes computationally derived hypotheses that warrant further validation through *in vitro*, *in vivo*, and pathway-level investigations to clarify biological relevance, target specificity, and potential off-target effects.

Author Contributions

Conceptualization, G.M.G., D.A., Y.A. and I.M.A.; methodology, G.M.G., D.A., Y.A. and I.M.A.; software, G.M.G. and I.M.A.; validation, G.M.G., D.A., Y.A. and I.M.A.; formal analysis, G.M.G., D.A., Y.A. and I.M.A.; investigation, G.M.G.; resources, G.M.G.; data curation, G.M.G., D.A., Y.A. and I.M.A.; writing—original draft preparation, G.M.G.; writing—review and editing, G.M.G., D.A., Y.A. and I.M.A.; visualization, G.M.G.; supervision, D.A., Y.A. and I.M.A. All authors have read and agreed to the published version of the manuscript.

Institutional Review Board Statement

Not applicable.

Informed Consent Statement

Not applicable.

Data Availability Statement

Data supporting the findings of this study are available upon reasonable request from the corresponding author.

Funding

This research received no external funding.

Acknowledgments

Some of the data from this study were presented at the 2nd International Seminar on Tropical Bioresources Advancement and Technology (ISOTOBAT 2025), held online on May 23, 2025. This work was carried out under the auspices of the Department of Biochemistry, IPB University, and the National Research and Innovation Agency.

Conflicts of Interest

The authors declare no conflict of interest.

References

1. Niveshika; Singh, S.; Verma, E.; Mishra, A.K. In silico molecular docking analysis of cancer biomarkers with GC/MS identified compounds of *Scytonema* sp. *Netw. Model. Anal. Health Informatics Bioinform.* **2020**, *9*, 30, <https://doi.org/10.1007/s13721-020-00235-w>.
2. Sun, X.; Hu, X. Unveiling Matrix Metalloproteinase 13's Dynamic Role in Breast Cancer: A Link to Physical Changes and Prognostic Modulation. *Int. J. Mol. Sci.* **2025**, *26*, 3083, <https://doi.org/10.3390/ijms26073083>.
3. Breast Cancer. Available online: <https://www.who.int/news-room/fact-sheets/detail/breast-cancer> (accessed on 5 January **2026**).
4. Azmi, A.S.; Wang, Z.; Philip, P.A.; Mohammad, R.M.; Sarkar, F.H. Emerging Bcl-2 inhibitors for the treatment of cancer. *Exp. Opin. Emerg. Drugs* **2011**, *16*, 59-70, <https://doi.org/10.1517/14728214.2010.515210>.
5. Suvarna, V.; Singh, V.; Murahari, M. Current overview on the clinical update of Bcl-2 anti-apoptotic inhibitors for cancer therapy. *Eur. J. Pharmacol.* **2019**, *862*, 172655, <https://doi.org/10.1016/j.ejphar.2019.172655>.
6. Alam, M.; Ali, S.; Mohammad, T.; Hasan, G.M.; Yadav, D.K.; Hassan, M.I. B Cell Lymphoma 2: A Potential Therapeutic Target for Cancer Therapy. *Int. J. Mol. Sci.* **2021**, *22*, 10442, <https://doi.org/10.3390/ijms221910442>.
7. Morelos-Garnica, L.-A.; Guzmán-Velázquez, S.; Padilla-Martínez, I.-I.; García-Sánchez, J.-R.; Bello, M.; Bakalara, N.; Méndez-Luna, D.; Correa-Basurto, J. In silico design and cell-based evaluation of two dual anti breast cancer compounds targeting Bcl-2 and GPER. *Sci. Rep.* **2023**, *13*, 17933, <https://doi.org/10.1038/s41598-023-43860-x>.
8. Ujlaky-Nagy, L.; Szöllösi, J.; Vereb, G. Disrupting EGFR–HER2 Transactivation by Pertuzumab in HER2-Positive Cancer: Quantitative Analysis Reveals EGFR Signal Input as Potential Predictor of Therapeutic Outcome. *Int. J. Mol. Sci.* **2024**, *25*, 5978, <https://doi.org/10.3390/ijms25115978>.
9. Wang, Y.; Minden, A. Current Molecular Combination Therapies Used for the Treatment of Breast Cancer. *Int. J. Mol. Sci.* **2022**, *23*, 11046, <https://doi.org/10.3390/ijms231911046>.
10. Spada, A.; Gerber-Lemaire, S. Surface Functionalization of Nanocarriers with Anti-EGFR Ligands for Cancer Active Targeting. *Nanomaterials* **2025**, *15*, 158, <https://doi.org/10.3390/nano15030158>.
11. Mariana Kustiawan, P.; Siregar, K.A.A.K.; Syaifie, P.H.; Zein Muttaqin, F.; Ibadillah, D.; Miftah Jauhar, M.; Djamas, N.; Mardiyati, E.; Taufiqu Rochman, N. Uncovering the anti-breast cancer activity potential of east Kalimantan propolis by In vitro and bioinformatics analysis. *Heliyon* **2024**, *10*, e33636, <https://doi.org/10.1016/j.heliyon.2024.e33636>.
12. Simanjuntak, M.V.; Jauhar, M.M.; Syaifie, P.H.; Arda, A.G.; Mardiyati, E.; Shalannanda, W.; Hermanto, B.R.; Anshori, I. Revealing Propolis Potential Activity on Inhibiting Estrogen Receptor and Heat Shock Protein 90 Overexpressed in Breast Cancer by Bioinformatics Approaches. *Bioinform. Biol. Insights* **2024**, *18*, 11779322231224187, <https://doi.org/10.1177/11779322231224187>.
13. Albalawi, A.E.; Althobaiti, N.A.; Alrdahe, S.S.; Alhasani, R.H.; Alaryani, F.S.; BinMowyna, M.N. Antitumor Activity of Royal Jelly and Its Cellular Mechanisms against Ehrlich Solid Tumor in Mice. *BioMed Res. Int.* **2022**, *2022*, 7233997, <https://doi.org/10.1155/2022/7233997>.
14. Zhang, D.; Yuan, Y.; Xiong, J.; Zeng, Q.; Gan, Y.; Jiang, K.; Xie, N. Anti-breast cancer effects of dairy protein active peptides, dairy products, and dairy protein-based nanoparticles. *Front. Pharmacol.* **2024**, *15*, 1486264, <https://doi.org/10.3389/fphar.2024.1486264>.

15. Hassan, A.A.-m.; Elenany, Y.E.; Nassrallah, A.; Cheng, W.; Abd El-Maksoud, A.A. Royal jelly improves the physicochemical properties and biological activities of fermented milk with enhanced probiotic viability. *LWT* **2022**, *155*, 112912, <https://doi.org/10.1016/j.lwt.2021.112912>.
16. Alnomasy, S.F.; Al Shehri, Z.S. Anti-cancer and cell toxicity effects of royal jelly and its cellular mechanisms against human hepatoma cells. *Pharmacogn. Mag.* **2022**, *18*, 635–640.
17. Sirkisoon, S.R.; Carpenter, R.L.; Rimkus, T.; Miller, L.; Metheny-Barlow, L.; Lo, H.-W. EGFR and HER2 signaling in breast cancer brain metastasis. *Front. Biosci.* **2016**, *8*, 245-263, <https://doi.org/10.2741/e765>.
18. Duda, M.; Velidandi, A.; Shyam Prasad, G. Novel pyrrole-chromone based chalcones: Synthesis and their anti-breast cancer activity: An *in-silico* study. *Res. Chem.* **2024**, *8*, 101560, <https://doi.org/10.1016/j.rechem.2024.101560>.
19. Rajagopal, K.; Kalusalingam, A.; Bharathidasan, A.R.; Sivaprakash, A.; Shanmugam, K.; Sundaramoorthy, M.; Byran, G. *In Silico* Drug Design of Anti-Breast Cancer Agents. *Molecules* **2023**, *28*, 4175, <https://doi.org/10.3390/molecules28104175>.
20. Sönmez, E. Royal Jelly in modern biomedicine: A review of its bioactive constituents and health benefits. *J. Funct. Foods* **2025**, *134*, 107062, <https://doi.org/10.1016/j.jff.2025.107062>.
21. Porter, J.; Payne, A.; de Candole, B.; Ford, D.; Hutchinson, B.; Trevitt, G.; Turner, J.; Edwards, C.; Watkins, C.; Whitcombe, I.; Davis, J.; Stubberfield, C. Tetrahydroisoquinoline amide substituted phenyl pyrazoles as selective Bcl-2 inhibitors. *Bioorg. Med. Chem. Lett.* **2009**, *19*, 230-233, <https://doi.org/10.1016/j.bmcl.2008.10.113>.
22. Stamos, J.; Sliwkowski, M.X.; Eigenbrot, C. Structure of the Epidermal Growth Factor Receptor Kinase Domain Alone and in Complex with a 4-Anilinoquinazoline Inhibitor*. *J. Biol. Chem.* **2002**, *277*, 46265-46272, <https://doi.org/10.1074/jbc.M207135200>.
23. Ishikawa, T.; Seto, M.; Banno, H.; Kawakita, Y.; Oorui, M.; Taniguchi, T.; Ohta, Y.; Tamura, T.; Nakayama, A.; Miki, H.; Kamiguchi, H.; Tanaka, T.; Habuka, N.; Sogabe, S.; Yano, J.; Aertgeerts, K.; Kamiyama, K. Design and Synthesis of Novel Human Epidermal Growth Factor Receptor 2 (HER2)/Epidermal Growth Factor Receptor (EGFR) Dual Inhibitors Bearing a Pyrrolo[3,2-*d*]pyrimidine Scaffold. *J. Med. Chem.* **2011**, *54*, 8030-8050, <https://doi.org/10.1021/jm2008634>.
24. Land, H.; Humble, M.S. YASARA: A Tool to Obtain Structural Guidance in Biocatalytic Investigations. In *Protein Engineering: Methods and Protocols*; Bornscheuer, U.T., Höhne, M., Eds.; Springer New York: New York, NY, **2018**; Volume 1685, pp. 43-67, https://doi.org/10.1007/978-1-4939-7366-8_4.
25. Kumar, M.; Rathore, R.S. *RamPlot*: a webserver to draw 2D, 3D and assorted Ramachandran (ϕ , ψ) maps. *J. Appl. Cryst.* **2025**, *58*, 630–636, <https://doi.org/10.1107/S1600576725001669>.
26. Liao, J.; Wang, Q.; Wu, F.; Huang, Z. *In Silico* Methods for Identification of Potential Active Sites of Therapeutic Targets. *Molecules* **2022**, *27*, 7103, <https://doi.org/10.3390/molecules27207103>.
27. Abdelhamid, S.A.; Mohamed, S.S.; Abo Elsoud, M.M.; Selim, M.S.; Mounier, M.M.; Eltaher, A.; Magdeldin, S.; Ali, M.; Awady, M.E.E. Characterization and Modeling of Marine *Bacillus cereus* Strain MSS1 Exopolysaccharide and Its Antagonistic Effect on Colon Cancer. *Probiotics Antimicrob. Proteins* **2025**, <https://doi.org/10.1007/s12602-025-10539-w>.
28. El-Seedi, H.R.; Salama, S.; El-Wahed, A.A.A.; Guo, Z.; Di Minno, A.; Daglia, M.; Li, C.; Guan, X.; Buccato, D.G.; Khalifa, S.A.M.; Wang, K. Exploring the Therapeutic Potential of Royal Jelly in Metabolic Disorders and Gastrointestinal Diseases. *Nutrients* **2024**, *16*, 393, <https://doi.org/10.3390/nu16030393>.
29. Botezan, S.; Baci, G.-M.; Bagameri, L.; Paşca, C.; Dezmirean, D.S. Current Status of the Bioactive Properties of Royal Jelly: A Comprehensive Review with a Focus on Its Anticancer, Anti-Inflammatory, and Antioxidant Effects. *Molecules* **2023**, *28*, 1510, <https://doi.org/10.3390/molecules28031510>.
30. Cavasotto, C.N.; Adler, N.S.; Aucar, M.G. Quantum Chemical Approaches in Structure-Based Virtual Screening and Lead Optimization. *Front. Chem.* **2018**, *6*, 188, <https://doi.org/10.3389/fchem.2018.00188>.
31. Moghtaderi, H.; Sadeghian, G.; Khan, F.; Rehman, N.U.; Halim, S.A.; Mohammadi, S.; Khan, A.; Gollahon, L.; Al-Harrasi, A.; Rahman, S.M. Flindersine from *Haplophyllum tuberculatum* modulates glycolysis and promotes apoptosis in breast cancer: Insights from *in vitro*, electrochemical, and molecular docking studies. *Pharmacol. Res. Nat. Prod.* **2025**, *9*, 100427, <https://doi.org/10.1016/j.prenap.2025.100427>.
32. Siguenza, J.; Baykara, H. Molecular docking and dynamics simulations of 4-heteroarylidenamino-4,5-dihydro-1H-1,2,4-triazol-5-one derivatives as potential anticancer agents. *Comput. Biol. Chem.* **2026**, *120*, 108657, <https://doi.org/10.1016/j.compbiolchem.2025.108657>.

33. Ozvoldik, K.; Stockner, T.; Krieger, E. YASARA Model–Interactive Molecular Modeling from Two Dimensions to Virtual Realities. *J. Chem. Inf. Model.* **2023**, *63*, 6177-6182, <https://doi.org/10.1021/acs.jcim.3c01136>.
34. Ridgway, H.; Moore, G.J.; Gadanec, L.K.; Matsoukas, J.M. Docking Simulations of G-Protein Coupled Receptors Uncover Crossover Binding Patterns of Diverse Ligands to Angiotensin, Alpha-Adrenergic and Opioid Receptors: Implications for Cardiovascular Disease and Addiction. *Biomolecules* **2025**, *15*, 855, <https://doi.org/10.3390/biom15060855>.
35. El fadili, M.; Er-Rajy, M.; Kara, M.; Assouguem, A.; Belhassan, A.; Alotaibi, A.; Mrabti, N.N.; Fidan, H.; Ullah, R.; Ercisli, S.; Zarougui, S.; Elhallaoui, M. QSAR, ADMET In Silico Pharmacokinetics, Molecular Docking and Molecular Dynamics Studies of Novel Bicyclo (Aryl Methyl) Benzamides as Potent GlyT1 Inhibitors for the Treatment of Schizophrenia. *Pharmaceutics* **2022**, *15*, 670, <https://doi.org/10.3390/ph15060670>.
36. Wako, H.; Endo, S. Normal mode analysis as a method to derive protein dynamics information from the Protein Data Bank. *Biophys. Rev.* **2017**, *9*, 877-893, <https://doi.org/10.1007/s12551-017-0330-2>.
37. Santra, D.; Maiti, S. Molecular dynamic simulation suggests stronger interaction of Omicron-spike with ACE2 than wild but weaker than Delta SARS-CoV-2 can be blocked by engineered S1-RBD fraction. *Struct. Chem.* **2022**, *33*, 1755-1769, <https://doi.org/10.1007/s11224-022-02022-x>.
38. Alsedfy, M.Y.; Ebnalwaled, A.A.; Moustafa, M.; Said, A.H. Investigating the binding affinity, molecular dynamics, and ADMET properties of curcumin-IONPs as a mucoadhesive bioavailable oral treatment for iron deficiency anemia. *Sci. Rep.* **2024**, *14*, 22027, <https://doi.org/10.1038/s41598-024-72577-8>.
39. onzález-Esparragoza, D.; Carrasco-Carballo, A.; Rosas-Murrieta, N.H.; Millán-Pérez Peña, L.; Luna, F.; Herrera-Camacho, I. In Silico Analysis of Protein–Protein Interactions of Putative Endoplasmic Reticulum Metallopeptidase 1 in *Schizosaccharomyces pombe*. *Curr. Issues Mol. Biol.* **2024**, *46*, 4609-4629, <https://doi.org/10.3390/cimb46050280>.
40. Turpo-Pequeña, A.G.; Leiva-Flores, E.K.; Luna-Prado, S.; Gómez, B. A Theoretical Study of the Interaction of PARP-1 with Natural and Synthetic Inhibitors: Advances in the Therapy of Triple-Negative Breast Cancer. *Curr. Issues Mol. Biol.* **2024**, *46*, 9415-9429, <https://doi.org/10.3390/cimb46090558>.
41. Mushebenge, A.G.-A.; Ugbaja, S.C.; Mbatha, N.A.; B. Khan, R.; Kumalo, H.M. Assessing the Potential Contribution of In Silico Studies in Discovering Drug Candidates That Interact with Various SARS-CoV-2 Receptors. *Int. J. Mol. Sci.* **2023**, *24*, 15518, <https://doi.org/10.3390/ijms242115518>.
42. Leis, S.; Schneider, S.; Zacharias, M. In Silico Prediction of Binding Sites on Proteins. *Curr. Med. Chem.* **2010**, *17*, 1550–1562, <https://doi.org/10.2174/092986710790979944>.
43. Ru, X.; Xu, L.; Han, W.; Zou, Q. In silico methods for drug-target interaction prediction. *Cell Rep. Methods* **2025**, *5*, 101184, <https://doi.org/10.1016/j.crmeth.2025.101184>.
44. Cheltsov, A. Q-MOL: High Fidelity Platform for In Silico Drug Discovery and Design. *bioRxiv* **2025**, 2025.2008.2006.668254, <https://doi.org/10.1101/2025.08.06.668254>.
45. Hasyim, D.M.; Musfiroh, I.; Hendra, R.; Fakhri, T.M.; Ikram, N.K.K.; Muchtaridi, M. In Silico Approaches for the Discovery of Novel Pyrazoline Benzenesulfonamide Derivatives as Anti-Breast Cancer Agents Against Estrogen Receptor Alpha (ER α). *Appl. Sci.* **2025**, *15*, 8444, <https://doi.org/10.3390/app15158444>.
46. Millan-Casarrubias, E.J.; García-Tejeda, Y.V.; González-De la Rosa, C.H.; Ruiz-Mazón, L.; Hernández-Rodríguez, Y.M.; Cigarroa-Mayorga, O.E. Molecular Docking and Pharmacological In Silico Evaluation of Camptothecin and Related Ligands as Promising HER2-Targeted Therapies for Breast Cancer. *Curr. Issues Mol. Biol.* **2025**, *47*, 193, <https://doi.org/10.3390/cimb47030193>.
47. Townsend, P.A.; Kozhevnikova, M.V.; Cexus, O.N.F.; Zamyatnin, A.A.; Soond, S.M. BH3-mimetics: recent developments in cancer therapy. *J. Exp. Clin. Cancer Res.* **2021**, *40*, 355, <https://doi.org/10.1186/s13046-021-02157-5>.
48. Alaseem, A.M.; Alasiri, G.; Babu, M.A.; Singh, T.G.; Alam, P.; Fareed, M.; Akhter, M.S.; Bansal, N. Employing a drug repurposing strategy to identify B-cell lymphoma-2 (BCL-2) inhibitors with anticancer potential: An in silico and in vitro based study. *Bioorg. Med. Chem.* **2025**, *130*, 118364, <https://doi.org/10.1016/j.bmc.2025.118364>.
49. Almansour, N.M.; Allemailem, K.S.; Abd El Aty, A.A.; Boussoufa, D.; Ismail Fagiree, E.; Ibrahim, M.A.A. Venetoclax analogs as promising anticancer therapeutics via targeting Bcl-2 protein: in-silico drug discovery study. *J. Biomol. Struct. Dyn.* **2023**, *41*, 14308-14324, <https://doi.org/10.1080/07391102.2023.2180668>.

50. Al Khzem, A.H.; Gomaa, M.S.; Alturki, M.S.; Tawfeeq, N.; Sarafroz, M.; Alonaizi, S.M.; Al Faran, A.; Alrumaihi, L.A.; Alansari, F.A.; Alghamdi, A.A. Drug Repurposing for Cancer Treatment: A Comprehensive Review. *Int. J. Mol. Sci.* **2024**, *25*, 12441, <https://doi.org/10.3390/ijms252212441>.
51. Bellino, S.; Lucente, D.; La Salvia, A. Drug Repurposing of New Treatments for Neuroendocrine Tumors. *Cancers* **2025**, *17*, 2488, <https://doi.org/10.3390/cancers17152488>.
52. Ghaffar, U.; Khan, F.; Hussain, J.; Mali, S.N.; Khan, A.; Chaudhari, S.Y.; Jawarkar, R.D.; Alanazi, A.K.; Islam, W.U.; Ismail, M.A.; Al-Harrasi, A.; Shafiq, Z. *In-vitro* and *in-silico* study to assess anti breast cancer potential of N-tosyl-indole based hydrazones. *Sci. Rep.* **2025**, *15*, 35733, <https://doi.org/10.1038/s41598-025-21326-6>.
53. Kaavin, K.; Naresh, D.; Yogeshkumar, M.R.; Krishna Prakash, M.; Janarthanan, S.; Murali Krishnan, M.; Malathi, M. *In-silico* DFT studies and molecular docking evaluation of benzimidazo methoxy quinoline-2-one ligand and its Co, Ni, Cu and Zn complexes as potential inhibitors of Bcl-2, Caspase-3, EGFR, mTOR, and PI3K, cancer-causing proteins. *Chem. Phys. Impact* **2024**, *8*, 100418, <https://doi.org/10.1016/j.chphi.2023.100418>.
54. Saritha, K.; Aivelu, M.; Mohammad, M. Drug-likeness analysis, in silico ADMET profiling of compounds in *Kedrostis foetidissima* (Jacq.) Cogn, and antibacterial activity of the plant extract. *In Silico Pharmacol.* **2024**, *12*, 67, <https://doi.org/10.1007/s40203-024-00240-1>.
55. Bauer, J.A.; Bauerová-Hlinková, V. Extracting the Dynamic Motion of Proteins Using Normal Mode Analysis Normal mode analysis (NMA). In *Data Mining Techniques for the Life Sciences*; Carugo, O., Eisenhaber, F., Eds.; Springer US: New York, NY, **2022**; Volume 2449, pp. 213-231, https://doi.org/10.1007/978-1-0716-2095-3_9.
56. Bhattacharya, K.; Bordoloi, R.; Chanu, N.R.; Kalita, R.; Sahariah, B.J.; Bhattacharjee, A. In silico discovery of 3 novel quercetin derivatives against papain-like protease, spike protein, and 3C-like protease of SARS-CoV-2. *J. Genet. Eng. Biotechnol.* **2022**, *20*, 43, <https://doi.org/10.1186/s43141-022-00314-7>.
57. Pourhajibagher, M.; Javanmard, Z.; Bahador, A. Molecular docking and antimicrobial activities of photoexcited inhibitors in antimicrobial photodynamic therapy against *Enterococcus faecalis* biofilms in endodontic infections. *AMB Express* **2024**, *14*, 94, <https://doi.org/10.1186/s13568-024-01751-y>.
58. Wang, Z.; Xu, S.; Lin, A.; Wei, C.; Li, Z.; Chen, Y.; Bie, B.; Liu, L. Targeting vascular dementia: Molecular docking and dynamics of natural ligands against neuroprotective proteins. *PLOS ONE* **2025**, *20*, e0331787, <https://doi.org/10.1371/journal.pone.0331787>.
59. Faheem, M.; Pandey, V.; Prasad, M.; Dixit, M. In-silico study of thiazolidinone-linked Glu-Ureido based PSMA ligands for PET application. *Discov. Chem.* **2025**, *2*, 323, <https://doi.org/10.1007/s44371-025-00403-9>.
60. Linani, A.; Bensenouci, S.; Hafsa, B.I.; Benarous, K.; Serseg, T.; Bou-Salah, L.; Alhatlani, B.Y. In Silico Investigation of Taurodispacamide A and Strepoxazine A from *Agelas oroides* S. as Potential Inhibitors of Neuroblastoma Targets Reveals Promising Anticancer Activity. *Appl. Sci.* **2024**, *14*, 9306, <https://doi.org/10.3390/app14209306>.
61. Elshafei, S.O.; Mahmoud, N.A.; Almofti, Y.A. Immunoinformatics, molecular docking and dynamics simulation approaches unveil a multi epitope-based potent peptide vaccine candidate against avian leukosis virus. *Sci. Rep.* **2024**, *14*, 2870, <https://doi.org/10.1038/s41598-024-53048-6>.

Publisher's Note & Disclaimer

The statements, opinions, and data presented in this publication are solely those of the individual author(s) and contributor(s) and do not necessarily reflect the views of the publisher and/or the editor(s). The publisher and/or the editor(s) disclaim any responsibility for the accuracy, completeness, or reliability of the content. Neither the publisher nor the editor(s) assume any legal liability for any errors, omissions, or consequences arising from the use of the information presented in this publication. Furthermore, the publisher and/or the editor(s) disclaim any liability for any injury, damage, or loss to persons or property that may result from the use of any ideas, methods, instructions, or products mentioned in the content. Readers are encouraged to independently verify any information before relying on it, and the publisher assumes no responsibility for any consequences arising from the use of materials contained in this publication.